ARTICLE

An Optimal Micropatterned End-Effecter for Enhancing Frictional Force on Large Intestinal Surface

Sung-Hoon Lee,[†,‡] Young-Tae Kim,[†,§] Sungwook Yang,[∥] Eui-Sung Yoon,[∥] Dae-Eun Kim,[*,§] and Kahp Y. Suh[*,‡,⊥]

School of Mechanical and Aerospace Engineering and Institute of Advanced Machinery and Design, Seoul National University, Seoul, 151-742, Korea, School of Mechanical Engineering, Yonsei University, Seoul, 120-749, Korea, and Nano-Bio Center, Korea Institute of Science and Technology, Seoul, 136-791, Korea

ABSTRACT We present a simple surface modification method for enhancing the frictional properties on soft, viscoelastic tissue of large intestine by integrating micropatterned structures with controlled shape and geometry. The micropatterned end-effecter (EE) was fabricated onto micromachined EE body (20 mm long, 2 mm diameter cylinders) in the forms of line, box, pyramid, and bottle shape by utilizing capillary molding technique with UV-curable poly(urethane acrylate) (PUA) polymer. To evaluate the frictional behavior of micropatterned EE, we employed a biotribotester, for easy loading and test of a biological organ specimen. It was found that the frictional properties of micropatterned EE are heavily dependent upon the shape of microstructure. The patterned EE with parallel lines (to the direction of locomotion) showed better frictional performance (average frictional coefficient ~1.53 and maximum ~3.98) compared with other micropatterned EEs (average frictional coefficient 0.72−0.94 and maximum 1.78−2.49) and nonpatterned EE (average frictional coefficient ~0.58 and maximum ~1.51). In addition, various geometric parameters (e.g., height, width, and space) as well as operating conditions (e.g., contact load and sliding speed) were systematically investigated for probing optimal anchoring function of the parallel line patterned EE.

KEYWORDS: friction • colon endoscope • microfabrication • end effector • surface patterning

INTRODUCTION

Micropatterned surfaces have been used in a variety of surface modification methods because of their unique and improved tribological properties toward wetting (1−4), adhesion (5−7), and friction (8, 9). Of these, the friction of a micropatterned surface has recently attracted great attention, especially with the development of micro/nanoelectromechanical systems (MEMS/NEMS) (10). In miniaturized systems, surface properties such as friction and stiction often restrict long-term durability and reliable operation of the devices (10, 11). To alleviate this intrinsic problem, researchers have developed surface modification either in the form of chemical treatment or topographical texturing, aiming to reduce the frictional resistance between contacting surfaces (10, 12, 13).

The need to control friction of micropatterned surfaces can be found in biomedical devices, in which friction needs to be (i) minimized for smooth and damage-free catheterization (14, 15) or (ii) maximized to generate a large traction force for active locomotion and navigation. In general, surface modification methods including coating with a hydrophilic polymer (16) and construction of micro/nanotopography on the catheter surface (14, 17) have been developed to reduce the frictional resistance. In some medical devices, however, an enhanced frictional force is needed to implement active locomotion of a device. A self-propelled colonoscope represents a typical example of such an active biomedical device. This colonoscope can travel from the anus to the descending colon in a self-locomotive and controlled manner for a less-stressful inspection (18, 19). For self-propelling, an effective locomotion strategy is a key to its successful performance and thus a number of elegant locomotion strategies have been proposed (20−24). However, it is difficult to generate a sufficient frictional force without tissue damage in part because of the complex working environment on the surface of large intestine. For example, the large intestinal surface is covered with a mucus layer, which acts as a lubricant and often brings about an extremely slippery surface (25). Furthermore, it is deformable and stretchable with viscoelastic behavior (26).

To enhance self-propelled locomotion, researchers have employed a friction-enhancing element, a so-called end-effecter (EE), on the actuation parts of the endoscope by using clampers (27, 28), microhooks (29), adhesive films (30), and micropatterns (31−34). Although these techniques are beneficial and can advance the locomotion performance, there are a number of drawbacks. For example, the tissues are prone to bleeding as a result of poking or puncture when clampers and microhooks are not properly utilized. A mu-

* Corresponding author. E-mail: sky4u@snu.ac.kr (K.Y.S.); kimde@yonsei.ac.kr (D.-E.K.).

Received for review October 21, 2009 and accepted April 13, 2010

† S.-H.L. and Y.-T.K. contributed equally to this work.

‡ School of Mechanical and Aerospace Engineering, Seoul National University.

§ Yonsei University.

∥ Korea Institute of Science and Technology.

⊥ Institute of Advanced Machinery and Design, Seoul National University.

DOI: 10.1021/am900723a

Published on Web 04/23/2010

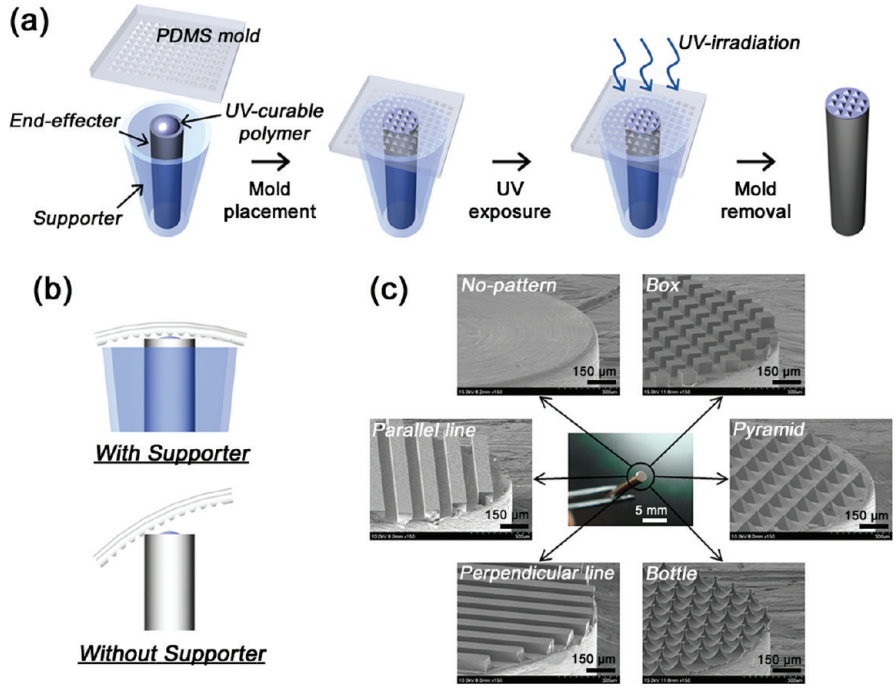

FIGURE 1. (a) Schematic illustration of the experimental procedure for fabricating a micropatterned end-effecter (EE) by capillary molding with UV-curable PUA resin. (b) Schematic illustration showing the role of supporter and thin PDMS mold for the conformal contact between PDMS mold and end surface of EE body. (c) Photograph of micropatterned EE together with magnified scanning electron microscope (SEM) images of various microstructures formed on EE surface. The dimension for each microstructure is 65 μm in height, 85 μm in width, and 65 μm in space, respectively.

coadhesive film can generate a high frictional force by the formation of molecular bonds (both covalent and noncovalent bonds) with the mucus layer. However, the material property should be altered to generate a relatively low frictional force by external stimuli such as pH, temperature, and shear rate for the detachment of a mucoadhesive from the mucus layer (35). In the case of using micropatterns, previous studies have demonstrated the ability to enhance the frictional force to a certain extent. Nevertheless, there has been no comprehensive study dealing with the effects of various geometric parameters (e.g., shape and dimension of micropatterns) and operating conditions (e.g., contact load and sliding speed). A major motivation with the use of a micropatterned EE is that one can take advantage of the enhanced frictional interactions together with minimal tissue damage at the expense of the remarkable anchoring capability of clampers and microhooks.

In this study, we present a simple method for fabricating micropatterned EE with optimized shape by utilizing capillary molding with a UV-curable polymer. The frictional behavior of micropatterned EE on the large intestinal surface was measured by a custom-built biotribotester, which had been specially designed with an *in vivo* like environment. On the basis of the measurement of frictional force, optimization of topographical shape of micropatterns, selection of magnitude of critical operating factors such as contact load and sliding speed, and identification of major frictional mechanisms were achieved. It is expected that a systematic investigation of these fundamental, biotribological parameters would give an insight into how a flat surface can be transformed into an effective EE for controlled physical contact and sliding motion on a complex tissue environment.

EXPERIMENTAL SECTION

Preparation of Silicon Masters and PDMS Molds. Silicon masters with box, perpendicular line, and parallel line microstructure were prepared by standard photolithography and deep reactive ion etching (RIE). A silicon master with pyramidal microstructure was fabricated by using anisotropic wet etching with 25% tetramethylammonium hydroxide (TMAH) solution, resulting in a slope angle of 54.7°. A silicon master with bottle shaped microstructure was prepared by isotropic etching with SF_6/O_2 gases in inductively coupled plasma (ICP) etcher. Polydimethylsiloxane (PDMS) molds were prepared by casting the PDMS prepolymer (Sylgard 184, Dow Corning) with 10% curing agent. For preparing a PDMS mold with pyramidal micro cavity, additional replication step was required as follows: (1) using UV-curable PUA polymer, pyramidal microstructures (features sticking out) were replicated onto transparent polyethylene terephthalate (PET) film from silicon master (features sticking in); (2) after peeling off the replica, additional UV irradiation was applied for removing trapped polymer radicals and unsaturated acrylate groups; (3) finally, a PDMS mold (features sticking in) was rereplicated by casting the PDMS prepolymer.

Fabrication of Micropatterned EE by UV-Assisted Capillary Molding. The micropatterned EE was fabricated by UV-assisted capillary molding method as shown in Figure 1a (36). In this method, an UV-curable resin of polyurethane acrylate (PUA, 311 RM, Minuta Tech) was used as the structural material. This material is useful for microfabrication in various aspects including its tunability of the mechanical properties (20−320 MPa in tensile modulus and 9−45% in elongation rate, respectively) and short curing time (tens of seconds). In our experiment, relatively hard PUA (320 MPa in tensile modulus and 9% in elongation rate, respectively) material was used due to its high structural integrity and easy processability (37). For the EE body, a cylindrical stainless steel pin was prepared with 2 mm diameter and 20 mm length. The fabrication procedure for generating micropatterned end-effecter can be divided into three steps: (1) a PDMS mold having engraved feature was uniformly placed on the drop-dispensed (~0.3 μL) UV-curable

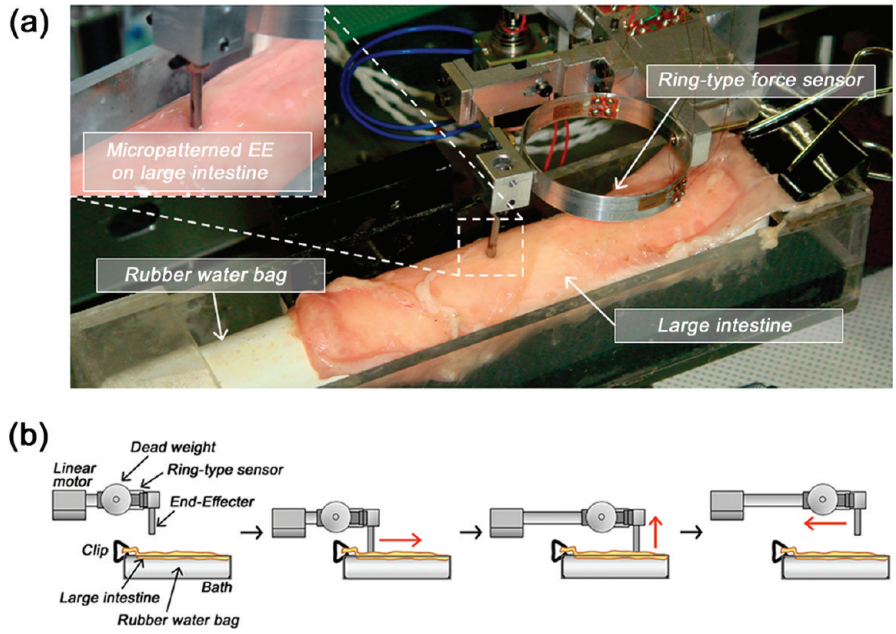

FIGURE 2. (a) Photograph of the custom-built biotribotester for measuring frictional force of micropatterned EE on the large intestinal surface. (b) Schematic illustration for the motion of micropatterned EE in an in vitro test. The mounted micropatterned EE is slid forward and backward driven by a linear motor.

PUA layer and a slight pressure (~0.2 g/cm^2) was applied for conformal contact; (2) after filling the polymer resin into the cavity of the mold by capillary action, the whole assembly was exposed to UV irradiation ($\lambda = 250-400$ nm) for ~40 s; (3) the PDMS mold was peeled from the EE body, leaving behind completely cured, polymeric microstructures.

To enable uniform pattern formation on EE body, conformal contact was needed due to a size difference between the PDMS mold (10 × 10 mm^2) and the end surface of EE body (2 mm in diameter). Therefore, the EE body was encapsulated by a supporter with the shape of hollow cylinder (inner diameter ~5 mm), so that the PDMS mold was placed adequately against the polymer layer without misalignment or nonuniform contact as schematized in Figure 1b. In addition, the use of a relatively thin PDMS mold (~2 mm) further improved conformal contact, owing to its excellent flexibility and wettability. Figure 1c shows fabrication results using the procedure described above, for which a detailed explanation is given shortly.

Preparation of Large Intestine Specimen of a Porcine. Large intestine specimen of a porcine was used for the friction tests. The specimen was transported from a slaughter house to the laboratory in a saline solution (NaCl 0.9%) just after being slaughtered and was used for the tests within 5–7 h. By doing this, surface degradation and changes in mechanical property of the specimen were largely suppressed. Also, the specimen was maintained to be wet by periodically sprinkling with the saline solution during the investigation.

Measurement of Frictional Force Using a Custom-Built Biotribotester. To measure the frictional force of micropatterned EE in an *in vitro* test, a custom-built biotribotester was specially designed as shown in Figure 2a. The large intestine specimen was cut into an appropriate size and placed on the rubber water bag inside the test bath. The rubber water bag was used to simulate the deformation property of the surrounding organs inside the body. One side of the large intestine was fixed with a clip and the opposite side was placed freely. Then, the micropatterned EE was connected to a ring type force sensor and then loaded on the large intestinal surface with a dead weight. Frictional force between the surfaces of micropatterned EE and large intestinal surface was measured by the force sensor during the relative motion, generated by a linear motor in the direction of the arrow, as shown in Figure 2b. In the experiment, the frictional force was measured three times in a row and averaged for a given micropatterned EE. In addition, the sliding speed was constantly controlled by the linear motor and a constant contact load was applied on the intestine surface by the counter dead weight. The contact load and sliding speed were varied from 2 to 5 and 10 gf, and from 2 to 5 and 10 mm/s, respectively, with a constant sliding distance of 25 mm.

Scanning Electron Microscopy (SEM). High-resolution SEM images were obtained using a HITACHI S-4800 microscope (Hitachi, Japan) operating at an accelerating voltage of 5 kV. To avoid charging effects, Au was sputter-coated to a thickness of 20 nm prior to imaging.

RESULTS

Fabrication of Micropatterned EE by UV-Assisted Capillary Molding. Figure 1c shows SEM images of various patterned microstructures on the end surface of the EE body (cylindrical stainless steel pin, 2 mm diameter and 20 mm length; see the center photograph) as well as the nonpatterned EE body (control). To investigate the frictional characteristic of micropatterned EE with different microstructure, five kinds of microstructures were used with the shapes of box, pyramid, bottle, perpendicular (to the direction of locomotion) line, and parallel (to the direction of locomotion) line. As shown in the figure, well-defined microstructures were fabricated on the end surface with good physical integrity. The adhesion between the microstructure and the EE body was relatively high, so that no appreciable delamination or distortion of the patterned layer was observed during repeated sliding motions. Although each microstructure has a different structural shape, the geometrical parameters such as height, width, and space were the same, which had been carefully designed (65 μm height, 85 μm width, and 65 μm space) by emulating the morphological dimension of biological attachment systems

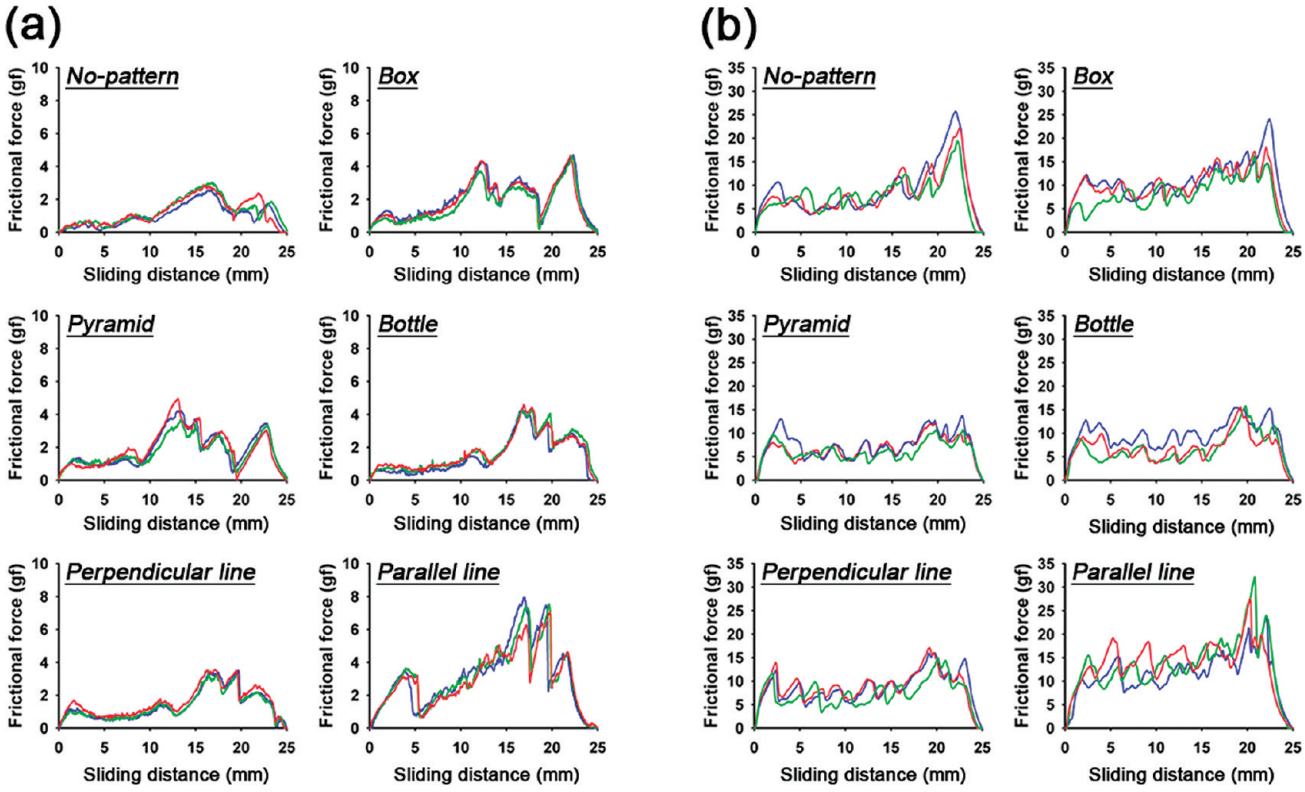

FIGURE 3. (a) Frictional behavior for micropatterned and nonpatterned EE on large intestine surface with 2 gf contact load, 5 mm/s sliding speed, and 25 mm sliding distance. (b) Frictional behavior for micropatterned and nonpatterned EE on large intestine surface with 10 gf contact load, 5 mm/s sliding speed, and 25 mm sliding distance. All the frictional force tests were performed at least three times on the same large intestine specimen.

such as *Taenia solium*, a typical parasite existing within the gastrointestinal tract (29).

It is worth noting that our soft lithographic approach to fabricate micropatterned EE is a simple and low-expertise route compared with other methods. For example, electrical discharge machining (EDM) is a useful technique, allowing for topographical modification of EE surface with high accuracy, even with a complex profile. However, a long turnaround time with limited working material (only electrically conductive material) restricts its widespread use (38). Replica molding is also a useful method but it requires additional assembling steps for integrating a micropatterned layer with the EE body (31).

Frictional Behavior of Various Micropatterned EE. In this study, the large intestine of a porcine was used as an organ specimen of the *in vitro* experimentation due to its similarity in shape, size, surface structure, and mechanical property to that of human body (39). Figure 3 shows the frictional behavior of various micropatterned EEs under (a) low and (b) high contact loads of 2 and 10 gf, respectively. In this experiment, the frictional forces were measured as a function of sliding distance at a constant sliding speed (5 mm/s) under two different contact loads. For statistical significance, the experiments were repeated at least three times for each EE using the same large intestine specimen.

As can be seen from the figure, under the low contact load (Figure 3(a)), the parallel line patterned EE gave a higher frictional force (average ~3.1 gf and maximum ~7.9 gf) as compared to that of nonpatterned EE (average ~1.2 gf and maximum ~3.0 gf) and those of other micropatterned EEs (average 1.4−1.9 gf and maximum 3.6−4.9 gf). Friction coefficients were obtained from the force data by dividing the frictional force by the applied load as defined by the Amonton's friction law. Remarkably, only the frictional coefficient for the parallel line patterned EE exceeded unity, potentially capable of generating an effective traction force on the large intestinal surface. It is noted that all the samples (including control) showed multiple peaks (2−4) with the peak locations being different with different patterns, which is a characteristic of typical stick-and-slip motion. In particular, only the parallel line patterned EE showed four peaks, of which the first peak set in at the sliding distance of ~4 mm. This fact suggests that the initial sliding motion of the parallel line patterned EE is quite unique, which can be interpreted as generating a high traction force within a short sliding distance. To assess the frictional behavior of the samples, the sliding motion of micropatterned EE was also observed using a typical vision system during the frictional force measurement. In the case of the high contact load (Figure 3b), there was no appreciable difference in the initial frictional force curves for all the microstructures tested. Also, the parallel line structure exhibited a slightly higher frictional force (average ~12.8 gf) over the total sliding distance than those of other micropatterned EEs (average 7.6−9.6 gf). In general, the friction profiles in Figure 3a were more pattern-dependent, which indicates that the small contact load regime is governed by a more complicated contact mecha-

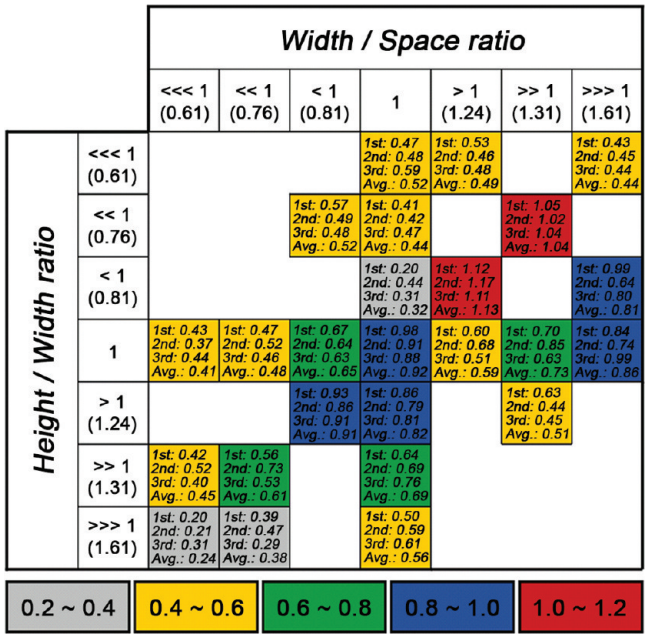

FIGURE 4. Friction coefficients for every three friction measurements and corresponding averaged friction coefficients of each parallel line patterned EE as functions of the height-to-width (H/W) and the width-to-space (*W*/*S*) ratios. All the frictional force tests were performed on the same large intestine specimen, under constant contact load (2 gf), sliding speed (5 mm/s), and sliding distance (25 mm).

nism involving a pattern-dependent, shallow deformation of the large intestinal tissue.

Evaluation of Geometric Parameters and Operating Conditions. On the basis of our experimental findings thus far, we provisionally conclude that the parallel line microstructure with respect to the locomotion direction is most effective in terms of high frictional coefficient. For further performance improvement, we evaluated the effect of geometric parameters for the parallel line patterned EE such as height, width, and space, as well as the operating conditions including contact load and sliding speed.

First, the friction coefficient was evaluated according to the variation in height, width, and space. For this experiment, each dimension of parallel line was varied as 65, 85, and 105 μm, resulting 27 different combinations. The contact load, sliding speed, and sliding distance were fixed at 2 gf, 5 mm/s, and 25 mm, respectively. Figure 4 shows the friction coefficients for every three friction measurements and corresponding averaged friction coefficients of each parallel line patterned EE as functions of the height-to-width (*H*/*W*) and the width-to-space (*W*/*S*) ratios. Because the initial frictional behavior is the key element for effective interlocking on the large intestine surface, the friction coefficient at the first peak was used for quantitative comparisons. As shown in the figure, with respect to two geometric ratios (*H*/*W* and *W*/*S*), the friction coefficient ranged from 0.24 to 1.13. In general, the coefficient became smaller as either one ratio (*H*/*W* or *W*/*S*) gets much smaller ($\ll$1) or larger ($\gg$1) than the other ratio. When the two ratios are comparable, the micropatterned EE rendered relatively larger friction coefficients of greater than 1. The specific parameters were: 0.81 for *H*/*W* and 1.23 for *W*/*S* and 0.76 for *H*/*W* and 1.31 for *W*/*S*.

Second, the effects of operating conditions were investigated for the parallel line patterned EE. Based on the above result, two effective parallel line microstructures were used: 65 μm height, 85 μm width, and 65 μm space for type A and 85 μm height, 105 μm width, and 85 μm space for type B. Figure 5a shows the frictional forces as well as the corresponding friction coefficients of the parallel line patterned EE as a function of contact load under a constant sliding speed of 5 mm/s. With an increase in the contact load from 2 to 10 gf, the forces for both EEs gradually increased in proportion to the increase of the contact load. In contrast, the corresponding friction coefficients decreased inversely to the contact load. Figure 5b shows the frictional forces and the corresponding friction coefficients as a function of sliding speed. Under a constant contact load of 2 gf, both frictional force and frictional coefficient were slightly increased with increasing the sliding speed from 2 through 5 to 10 mm/s. However, the frictional behavior was not so sensitive as compared to that for the contact load.

DISCUSSION

Usefulness and Limitation of the *In vitro* Friction Test. To assess the frictional performance of the micropatterned EE, we conducted *in vitro* friction tests by employing a custom-built biotribotester. A few comments are in order as to why such an *in vitro* test would be useful for potential applications in the locomotion of a self-propelled colonoscope inside the large intestinal tract. In real situations, the colonoscope should overcome both the frictional and geometrical resistances inside the large intestine. If the colonoscope with a micropatterned EE is directly inserted into an organ specimen as in an *in vivo* test, it is difficult to decouple the contributions from the entire shape of colonoscope and the shape of micropatterned EE, both of which can affect the frictional properties. More specifically, when the two resistances are comparable, the friction of the micropatterned EE cannot be properly evaluated. Therefore, it is necessary to separate the micropatterned EE from the total system to evaluate the frictional effect of micropatterned EE alone. In addition, the *in vitro* test makes it possible to evaluate the frictional performance under various operating conditions in terms of contact load and sliding speed.

However, there are some limitations and difficulties arising from the *in vitro* test. First, the measurement of friction properties depends not only on the topography of micropattern but also on the topography of the large intestinal surface. Furthermore, care should be taken so as to prevent the surface degradation and change in the mechanical properties of the large intestine, which can significantly affect the frictional behavior. To avoid this problem, for a given set of experiments, we used a single fresh intestine specimen to allow for systematic comparison (e.g., a set of experiments for investigating shape effects under 2 gf contact load). Second, the surface of large intestine may be possibly damaged by the repeating sliding motion. To

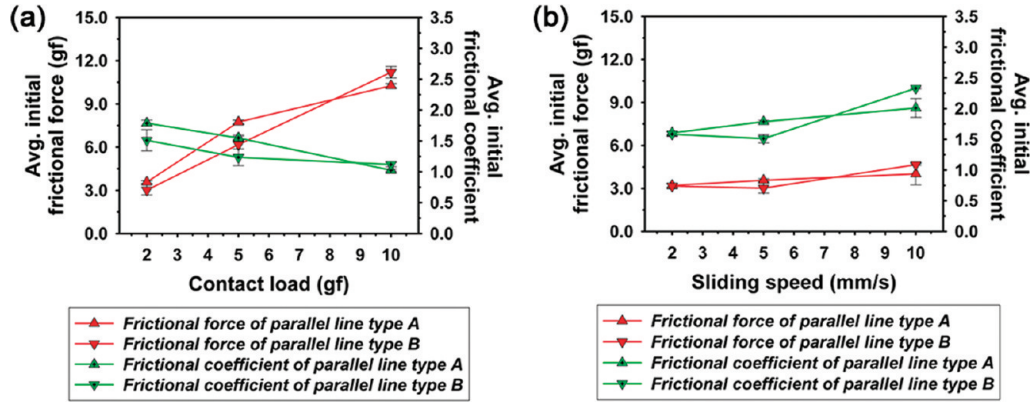

FIGURE 5. (a) Averaged initial frictional force and corresponding friction coefficient for two effective parallel line patterned EEs as a function of contact load. The applied contact loads were 2, 5, and 10 gf, under a constant sliding speed of 5 mm/s and a sliding distance of 25 mm. (b) Averaged initial frictional force and corresponding friction coefficient for two effective parallel line patterned EEs as a function of sliding speed. The sliding speeds were 2, 5, and 10 mm/s under a constant contact load of 2 gf and a sliding distance of 25 mm. The dimensions of the parallel lines for type A and B are 65 μm in height, 85 μm in width, and 65 μm in space and 85 μm in height, 105 μm in width, and 85 μm in space, respectively. All the frictional force tests were performed at least three times on the same large intestine specimen.

minimize this effect, we designed the experimental procedure with the intention of maintaining systematic and consistent comparison among the micropatterned EE while minimizing the influence of altered surface state of the intestine specimen on the frictional behavior. That is, a relatively low load was used in the friction test and the number of experiment repeated was restricted to only 3 in most cases. Third, during the sliding motion, a portion of the mucosal layer may be trapped into the grooves, which can possibly affect the subsequent measurement with repeated use of the same patterned surface. For this issue, it may be stated that the amount of mucus that existed on the intestine surface was insignificant and therefore, the lubrication effect of mucus was not a concern as judged by the fact that the three measurements gave quite consistent results.

Advantage of Micropattern for Effective Interlocking on Intestinal Surface. In previous works, physical interlocking has been proposed as one of the solutions for generating effective traction force on intestinal surface. In addition, the development of effective interlocking mechanism with minimized surface damage has also been a challenging task. A hook-worm is a good example to see how physical interlocking mechanism can be used to create locomotion on intestinal surface. However, to generate motion of a device as large as the self-propelled colonoscope that is being targeted in this work, the interlocking force has to be significant. If such a force were to be created using a wedgelike sharp tip, the intestinal wall would be readily damaged. Thus, the basic hypothesis of using the micropatterned structures was that they can be effectively interlocked with the intestinal surface while not imparting significant damage to the intestinal surface. The reasoning behind this hypothesis is that the micropatterns would be effective in distributing the interlocking force over a larger area, thus lowering the penetration pressure at each interlocking point. As for the specific shapes and dimensions of the micropatterns, they were determined partly from intuition and partly from preliminary experiments. Basically, the height of the micropattern structure has to be large enough to cause the interlocking effect but small enough so that they can be readily fabricated. Also, the gap between the structures of the patterns need to be large enough to allow the tissue to be squeezed in but small enough so that sufficient number of interlocking points can be achieved within a given area.

Frictional Performance of Various Micropatterned EEs. As shown in Figure 3, the measured friction forces showed distinctively different behavior with respect to the contact load applied to the EE. In particular, under the low contact load (2 gf), several notable findings can be derived. First, during the repeating measurements for each sample, all the frictional force curves showed a very similar profile with nearly the same peak locations. It appears that for a given geometry, each EE sticks and slides nearly at the same locations while interacting with the intrinsic surface topography of the large intestine specimen. As a consequence, use of a different EE gives rise to a different profile as shown in Figure 3a, which is determined by the local frictional interaction with the structural variation of the large intestinal surface. Second, the initial frictional behavior is important to judge which microstructure can effectively generate a large frictional force for interlocking. This is because a miniaturized self-propelled colonoscope usually has a limited stroke range and thus the ability to generate a high traction force within a short sliding distance is of great importance. As shown in Figure 3a, the parallel line patterned EE shows the highest initial frictional force of about 3.5 gf within the first 5 mm sliding distance, whereas the other microstructures show relatively lower forces of about 1 gf. Third, the friction forces of all the microstructures, except for the parallel line, were enhanced at around 10−15 mm sliding distance despite the fact that these microstructures did not show a first peak or a high initial force. It appears that the large intestinal surface is readily pushed and deformed forward by the lateral motion of the micropatterned EE. Because of the viscoelastic property of the intestinal tissue, some tissue material is accumulated ahead of the sliding micropatterned EE. Such a mass pile-up becomes significant at around 10−20 mm sliding distance, which in turn gives a higher geometric resistance regardless

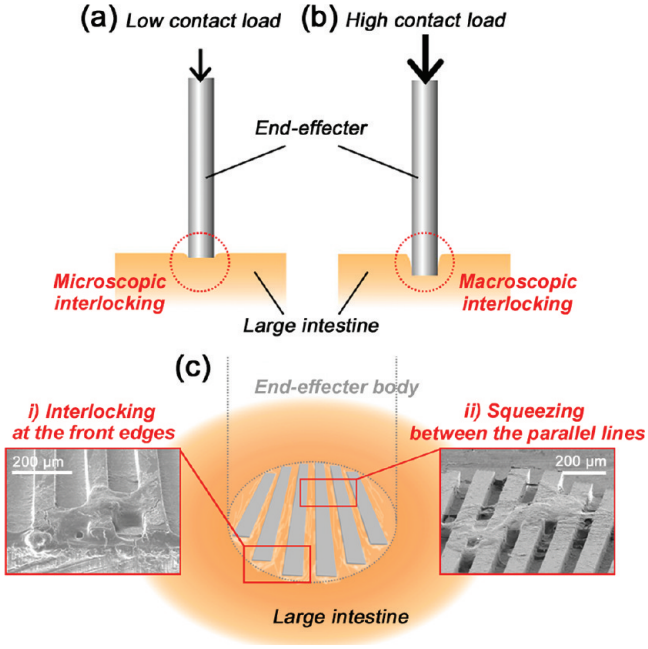

FIGURE 6. Schematic illustration of the cross-sectional contact geometries between the micropatterned EE and the large intestine surface under (a) a low contact load and (b) a high contact load. (c) A graphical illustration for two main friction generating mechanisms of parallel line patterned EE. The high contact pressure is generated at the front edge of parallel lines (interlocking effect) and the large intestine tissue is squeezed between parallel lines (squeezing effect) along the lateral sliding motion of micropatterned EE. The inserted SEM images show the intestine tissues at the front edges and inside the spaces of parallel line microstructures after the friction tests.

of the pattern shape. For the parallel line structure, the first peak appears within 5 mm sliding presumably associated with initial physical interlocking and then the force continuously increases up to the maximum sliding distance of 25 mm with high stiction. These observations suggest that the parallel line microstructure is most effective in terms of high initial stiction and average friction coefficient.

Mechanism for Physical Interlocking between Micropatterned EE and Intestinal Surface. Although the friction mechanism between the micropatterned EE and the large intestinal surface seems complicated, the major role of patterned microstructures can be attributed to two factors: interlocking and squeezing. Deformation of the intestine tissue occurs when the contact pressure is relatively high. The deformation can cause interlocking of the contacted tip or edge on the intestine tissue, or puncture the tissue if its magnitude exceeds the strength of the tissue. The amount of interlocking depends on the magnitude of contact pressure or loading force, and therefore, the geometrical interlocking between surfaces changes under different contact loading conditions.

As illustrated in Figure 6a, under the low contact load of 2 gf, the micropatterned EE is brought into contact with the large intestine surface causing a shallow deformation of the mucosal layer. Thus, the frictional force is dominated by the microscopic interlocking that is related to microscale surface topography on the patterned EE. The parallel line microstructure shows the highest frictional force of all the microstructures tested as shown in Figure 3a. With enhanced stick–slip motion, the average friction coefficient was larger than 1.5. The interlocking is mainly generated at two locations of the front edge and space of parallel line microstructures as schematized in Figure 6c. When the micropatterned EE slides laterally, a high contact pressure is generated at the front edge of the parallel line microstructures. In addition, the mucosal layer is squeezed into the spaces between the parallel structures. The inserted SEM images in Figure 6c show a detached tissue layer at the front edge as well as in the spaces between microstructures after the friction test, supporting our claims that physical interlocking at the front edge and squeezing between the parallel lines appear as the main friction mechanisms under a low contact load.

It should be noted that the intestinal tissue would not be severely damaged by the above interlocking and squeezing effects. The maximum height of the parallel line microstructure is 85 μm and the thickness of the outermost intestinal surface or the mucosal layer is about 700 μm (39). Therefore, the penetration into the submucosal layer, which contains blood vessels and limp nodes, seems implausible. In views of noninvasive and damageless locomotion inside the large intestine, the parallel line patterned EE is indeed appropriate and provides advantages over other attachment mechanisms such as hooks and wedgelike sharp tips.

Under the high contact load of 10 gf, the frictional force is dominated by a large deformation of the intestinal tissue as shown in Figure 6b. Thus the interlocking between the EE and the intestinal surface occurs over a large contact area, in full contact with the end surface of the EE. As a result, a much higher force is needed to move the EE laterally. The EE has to continuously deform the surrounding tissue to overcome the geometrical resistance originating from the recovery force of the deformed tissue due to its viscoelastic property. Thus, under a high contact load, the frictional force is significantly affected by the large, macroscopic deformation of the intestine tissue and not so much by microscopic interlocking of the micropatterns. As a consequence, the frictional behaviors of all the EE specimens are similar under the high contact load of 10 gf as shown in Figure 3b. From these results, it can be concluded that the parallel line micropatterned EE would be most effective to generate a high frictional force for both micro- and macroscopic multiscale contact geometry on the intestine surface.

Evaluation of Geometric Parameters and Operating Conditions. As described earlier, the frictional behavior of the parallel line patterned EE can be explained based on the combined effect of geometry and material property of the large intestine. During the sliding motion, the large intestinal tissue is readily deformed into the spaces between parallel line structures, with its amount depending on the opening size and local contact pressure. Especially at the edge of the strips the contact pressure is locally concentrated, which in turn gives a high frictional force. Therefore, a smaller opening size or a smaller space would result in a higher friction coefficient. In contrast, when the distance between the strips becomes too small, the squeez-

ing effect would be diminished as the surface roughness of intestinal tissue becomes similar to or larger than the opening size. On the basis of this competing effect, we can determin a suitable ratio of *W*/*S*, which ranged from 1.24 to 1.31 for the conditions used in our experiments (Figure 4). In a similar fashion, the interplay between the height and width of the strips can be reasoned for effective squeezing; a suitable *H*/*W* ratio shows a narrow span of 0.76−0.81, revealing that the height needs to be smaller than the width, but sufficiently big for squeezing of the mucosal layer. However, if the height is too big for a given width the stiffness of the pattern may be too low to generate sufficient squeezing force needed to grab the intestinal tissue. Thus, an appropriate H/W ratio is necessary to create the interlocking effect. For the above selected geometric ratios, the friction coefficient turned out to be larger than unity.

Regarding the evaluation of contact load, the frictional force increases with the increase in contact load as shown in Figure 5a. This is readily understood in that the deformation of the intestinal tissue will increase because of deep penetration of the EE under a high load. Interestingly, the friction coefficient shows the opposite behavior of, decreasing frictional force with increasing of contact load. On the basis of these observations, a lower contact load seems advantageous considering the limited magnitude of contact load that can be exerted by a miniaturized colonoscope. As for the effect of sliding speed on the frictional behavior of the intestine, it is quite complicated because of the viscoelastic properties of the intestine. It is well-known that the mechanical behavior of viscoelastic materials depend on the strain rate. Because the sliding speed of the micropatterned EE corresponds to the strain rate, we can hypothesize that the frictional force change with the sliding speed of EE. However, it was found that the change of frictional force was not significant for the range of sliding speed tested in our experiment. A plausible explanation for this outcome is that the range of sliding speed variation was not large enough to verify the hypothesis. Because the range of sliding speed used in this work restricted within the design specification of the end-effecter actuator of the self-propelled colonoscope, the frictional force was not tested at a wider range of speed. A further study would be required to better understand the effect of speed on viscoelastic frictional behavior of the intestine.

CONCLUSIONS

An optimized micropatterned end-effecter (EE) has been presented toward enhancing the anchoring function on large intestine surface with potential applications to self-propelled locomotion and navigation of a miniaturized colonoscope. By utilizing capillary molding method with UV-curable PUA polymer, various micropatterned EEs were fabricated in a one-step process without any complicated or expensive equipment. Based on the measurement of friction coefficient via a custom-built biotribotester in an *in vivo* like environment, the parallel line patterned EE showed the best frictional performance (average friction coefficient ∼1.53 and maximum ∼3.98) compared with the control surface of nonpatterned EE as well as other micropatterned EEs. It was found that the interlocking with the intestinal tissue at the front edge and the squeezing in the space of the strips can provide the high stick−slip motion, including the high initial friction force within a short sliding distance (<5 mm). In addition, the effects of geometrical parameters (height, width, and space) and operating conditions (contact load and sliding speed) were systematically investigated for further improvement. On the basis of our experimental findings, the parallel line patterned EE, with geometric ratios of 0.81 (for *H*/*W*) and 1.23 (for *W*/*S*) or 0.76 (for *H*/*W*) and 1.31 (for *W*/*S*), exhibited the largest friction coefficient (>1), potentially capable of generating an effective traction force on large intestinal surface. As for operating conditions, the friction force was increased in proportional to the contact load, whereas the corresponding friction coefficient was inversely proportional to the contact load. Furthermore, there were no significant changes with respect to the change of sliding speed under a constant contact load.

Our study would be useful in several aspects. First, the fabrication method is simple and based on well-established soft lithography, allowing for a low-expertise route to surface modification for high frictional performance. Second, the use of an in vitro biotribotester offers an *in vivo* like working environment, whereas decoupling the mixed contribution from geometrical and frictional resistances in an *in vivo* test. This custom-made measuring device also enables evaluation of the frictional performance under various operating conditions (contact load, sliding speed). Third, an effective geometry for high-performance EE has been identified. Fourth, the frictional mechanism proposed in this work would be generalized to other biological tissues. Furthermore, it would also be useful for gaining fundamental understanding of friction mechanisms on viscoelastic substrate involving creep, stress relaxation, and hysteresis as well as for designing medical devices that encounter contact with biological materials.

Acknowledgment. This work was supported by the Intelligent Microsystem Center (IMC; http://www.microsystem.re.kr), which carries out one of the 21st century's Frontier R&D Projects sponsored by the Korea Ministry of Knowledge Economy. This work was also supported in part by the Grant-in-Aid for Next-Generation New Technology Development Programs (10030046) sponsored by the Korea Ministry of Knowledge Economy and the WCU (World Class University) program through the Korea Science and Engineering Foundation sponsored by the Ministry of Education, Science and Technology (R31-2008-000-10083-0).

REFERENCES AND NOTES

(1) Nosonovsky, M.; Bhushan, B. *Adv. Funct. Mater.* **2008**, *18*, 843–855.
(2) Gao, S. Y.; Li, Z. D.; Yang, S. X.; Jiang, K.; Li, Y.; Zeng, H. B.; Li, L.; Wang, H. Q. *ACS Appl. Mater. Interfaces* **2009**, *1*, 2080–2085.
(3) Jeong, H. E.; Lee, S. H.; Kim, J. K.; Suh, K. Y. *Langmuir* **2006**, *22*, 1640–1645.
(4) Liu, H. Q.; Szunerits, S.; Pisarek, M.; Xu, W. G.; Boukherroub, R. *ACS Appl. Mater. Interfaces* **2009**, *1*, 2086–2091.
(5) Jeong, H. E.; Lee, J. K.; Kim, H. N.; Moon, S. H.; Suh, K. Y. *Proc. Natl. Acad. Sci. U.S.A.* **2009**, *106*, 5639–5644.

(6) Murphy, M. P.; Kim, S.; Sitti, M. *ACS Appl. Mater. Interfaces* **2009**, *1*, 849–855.
(7) Kim, T. I.; Jeong, H. E.; Suh, K. Y.; Lee, H. H. *Adv. Mater.* **2009**, *21*, 2276–2281.
(8) Varenberg, M.; Gorb, S. N. *Adv. Mater.* **2009**, *21*, 483–486.
(9) Shirtcliffe, N. J.; McHale, G.; Newton, M. I.; Zhang, Y. *ACS Appl. Mater. Interfaces* **2009**, *1*, 1316–1323.
(10) Maboudian, R.; Carraro, C. *Annu. Rev. Phys. Chem.* **2004**, *55*, 35–54.
(11) Wang, W. Y.; Wang, Y. L.; Bao, H. F.; Xiong, B.; Bao, M. H. *Sens. Actuators, A* **2002**, *97—8*, 486–491.
(12) Bandorf, R.; Paulkowski, D. M.; Schiffmann, K. I.; Kuster, R. L. A. *J. Phys.: Condens. Matter* **2008**, *20*, 354018.
(13) Jung, Y. C.; Bhushan, B. *Nanotechnology* **2006**, *17*, 4970–4980.
(14) Jones, D. S.; Garvin, C. P.; Gorman, S. P. *Biomaterials* **2004**, *25*, 1421–1428.
(15) Takashima, K.; Shimomura, R.; Kitou, T.; Terada, H.; Yoshinaka, K.; Ikeuchi, K. *Tribol. Int.* **2007**, *40*, 319–328.
(16) Nagaoka, S.; Akashi, R. *Biomaterials* **1990**, *11*, 419–424.
(17) Sjong, A. *Adv. Mater. Process.* **2009**, *167*, 41–42.
(18) Phee, S. J.; Ng, W. S.; Chen, I. M.; SeowChoen, F.; Davies, B. L. *IEEE Eng. Med. Biol. Mag.* **1997**, *16*, 85–96.
(19) Vucelic, B.; Rex, D.; Pulanic, R.; Pfefer, J.; Hrstic, I.; Levin, B.; Halpern, Z.; Arber, N. *Gastroenterology* **2006**, *130*, 672–677.
(20) Park, S.; Park, H.; Park, S.; Kim, B. *J. Mech. Sci. Technol.* **2006**, *20*, 1012–1018.
(21) Peirs, J.; Reynaerts, D.; Van Brussel, H. *Sens. Actuatord, A* **2001**, *92*, 343–349.
(22) Phee, L.; Accoto, D.; Menciassi, A.; Stefanini, C.; Carrozza, M. C.; Dario, P. *IEEE Trans. Biomed. Eng.* **2002**, *49*, 613–616.
(23) Quirini, M.; Menciassi, A.; Scapellato, S.; Dario, P.; Rieber, F.; Ho, C. N.; Schostek, S.; Schurr, M. O. *Gastrointest. Endosc.* **2008**, *67*, 1153–1158.
(24) Quirini, M.; Menciassi, A.; Scapellato, S.; Stefanini, C.; Dario, P. *IEEE/ASME Trans. Mechatronics* **2008**, *13*, 169–179.
(25) Wang, K. D.; Yan, G. Z. *Meas. Sci. Technol.* **2009**, *20*, 015803.
(26) Kim, J. S.; Sung, I. H.; Kim, Y. T.; Kwon, E. Y.; Kim, D. E.; Jang, Y. H. *Tribol. Lett.* **2006**, *22*, 143–149.
(27) Menciassi, A.; Moglia, A.; Gorini, S.; Pernorio, G.; Stefanini, C.; Dario, P. *J. Micromech. Microeng.* **2005**, *15*, 2045–2055.
(28) Dejeu, J.; Gauthier, M.; Rougeot, P.; Boireau, W. *ACS Appl. Mater. Interfaces* **2009**, *1*, 1966–1973.
(29) Menciassi, A.; Dario, P. *Philos. Trans. R Soc. London, Ser. A* **2003**, *361*, 2287–2298.
(30) Dodou, D.; Breedveld, P.; Wieringa, P. A. *J. Appl. Phys.* **2006**, *100*, 014904.
(31) Glass, P.; Cheung, E.; Sitti, M. *IEEE Trans. Biomed. Eng.* **2008**, *55*, 2759–2767.
(32) Kim, S.; Aksak, B.; Sitti, M. *Appl. Phys. Lett.* **2007**, *91*, 221913.
(33) Kwon, J.; Cheung, E.; Park, S.; Sitti, M. *Biomed. Mater.* **2006**, *1*, 216–220.
(34) Majidi, C.; Groff, R. E.; Maeno, Y.; Schubert, B.; Baek, S.; Bush, B.; Maboudian, R.; Gravish, N.; Wilkinson, M.; Autumn, K.; Fearing, R. S. *Phys. Rev. Lett.* **2006**, *97*, 076103.
(35) Dodou, D.; Breedveld, P.; Wieringa, P. A. *Eur. J. Pharm. Biopharm* **2005**, *60*, 1–16.
(36) Suh, K. Y.; Park, M. C.; Kim, P. *Adv. Funct. Mater.* **2009**, *19*, 2699–2712.
(37) Choi, S. J.; Yoo, P. J.; Baek, S. J.; Kim, T. W.; Lee, H. H. *J. Am. Chem. Soc.* **2004**, *126*, 7744–7745.
(38) Cao, D. M.; Jiang, J.; Meng, W. J.; Jiang, J. C.; Wang, W. *Microsyst. Technol.* **2007**, *13*, 503–510.
(39) Mills, S. E. *Histology for Pathologists*; Lippincott Williams & Wilkins: Philadelphia, 2007.

AM900723A